ACS chemical biology

Letters

pubs.acs.org/acschemicalbiology

Large Scale Mutational and Kinetic Analysis of a Self-Hydrolyzing Deoxyribozyme

V. Dhamodharan, Shungo Kobori, and Yohei Yokobayashi*

Nucleic Acid Chemistry and Engineering Unit, Okinawa Institute of Science and Technology Graduate University, Onna, Okinawa 9040495, Japan

Supporting Information

ABSTRACT: Deoxyribozymes are catalytic DNA sequences whose atomic structures are generally difficult to elucidate. Mutational analysis remains a principal approach for understanding and engineering deoxyribozymes with diverse catalytic activities. However, laborious preparation and biochemical characterization of individual sequences severely limit the number of mutants that can be studied biochemically. Here, we applied deep sequencing to directly measure the activities of self-hydrolyzing deoxyribozyme sequences in high throughput. First, all single and double mutants within the 15-base catalytic core of the deoxyribozyme I-R3 were assayed to unambiguously determine the tolerated and untolerated mutations at each position. Subsequently, 4096 deoxyribozyme variants with tolerated base substitutions at seven positions were kinetically assayed in parallel. We identified 533 active mutants whose first-order rate constants and activation energies were determined. The results indicate an isolated and narrow peak in the deoxyribozyme sequence space and provide a quantitative view of the effects of multiple mutations on the deoxyribozyme activity for the first time.

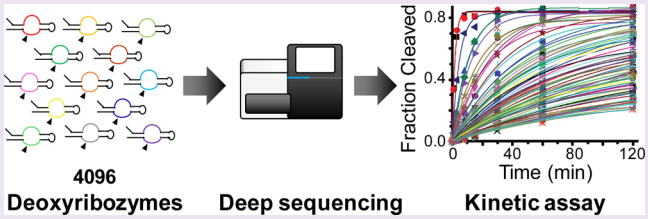

Deoxyribozymes are single-stranded DNA with catalytic function.[1,2] Unlike their RNA counterparts (ribozymes), deoxyribozymes have not been found in nature. However, laboratory selection and evolution efforts have yielded deoxyribozymes that can catalyze diverse chemical reactions such as DNA/RNA cleavage,[3,4] amide hydrolysis,[5] and the Diels−Alder reaction,[6] prompting interests in their basic chemistry as well as potential applications.[7−9] On the other hand, our structural and mechanistic understanding of deoxyribozymes is still limited. For example, while 3D structures of many ribozyme classes have been elucidated, only one deoxyribozyme crystal structure has been reported to date.[10] In the absence of precise structural information, biochemical methodologies remain a principal approach to understand and engineer deoxyribozymes. In particular, mutational analysis is indispensable for identifying catalytically and structurally important nucleotides.[11−15] However, conventional mutational analysis requires design, preparation, and evaluation of individual mutants, which is time-consuming and costly. Therefore, only a small number of arbitrarily chosen mutants are typically studied experimentally.

A significant advance in parallel mutational analysis of deoxyribozymes was achieved when Höbartner and co-workers reported a combinatorial scanning mutagenesis method that was used to identify functionally critical nucleotides in deoxyribozymes.[16−19] While this method offers an important advantage of allowing atomic mutagenesis,[17] it requires laborious combinatorial DNA synthesis, radiolabeling, and single-nucleotide resolution gel electrophoresis. Moreover, the assay can be applied to just single mutants and only affords qualitative "interference" factors. Therefore, a new analytical methodology that enables quantitative and high-throughput characterization of deoxyribozyme mutants should greatly contribute to fundamental investigations and applications of deoxyribozymes.

Earlier efforts to infer the fitness landscapes of in vitro selected nucleic acid enzymes relied on low-throughput Sanger sequencing[20] and targeted mutagenesis.[21] Deep sequencing technology has emerged as a powerful tool to unravel the fitness landscape of functional nucleic acids. For example, deep sequencing was used to analyze in vitro selection experiments to gain insights into the fitness landscapes of ribozymes[22−24] and aptamers.[25] Niland et al. determined the substrate sequence specificity of ribonuclease P by deep sequencing.[26] We recently used deep sequencing for high-throughput assay of ribozyme variants without selection.[27−29]

In the present work, we applied deep sequencing to perform large scale mutational profiling of a deoxyribozyme, which unambiguously identified catalytically essential nucleotides as well as tolerated mutations at every position. Furthermore, we demonstrated for the first time, a high-throughput kinetic analysis in which 4096 deoxyribozyme reactions were simultaneously assayed at multiple time points to calculate observed rate constants (k_{obs}) of 533 active deoxyribozyme mutants. The rate constants were used to calculate the activation energies (E_a) providing quantitative insights into the mutational landscape of the deoxyribozyme. To our

Received: July 23, 2017
Accepted: October 23, 2017
Published: October 23, 2017

DOI: 10.1021/acschembio.7b00621
ACS Chem. Biol. 2017, 12, 2940−2945

knowledge, such quantitative and high resolution mapping of the mutational landscape of nucleic acid enzymes has not been reported.

In this work, we focused on a Zn^{2+}-dependent deoxyribozyme called I-R3 that catalyzes DNA hydrolysis, discovered by the Breaker group through in vitro selection.[30] DNA hydrolysis catalyzed by DNA was first reported by the Silverman group while attempting to isolate deoxyribozymes with amide hydrolysis activity.[3] The distinct and compact catalytic core of I-R3 was discovered by a unique selection method that allows cleavage to occur at any position within the randomized sequence. The catalytic core of I-R3 is characterized by an asymmetric internal loop with 10 nucleotides on one side and 7 nucleotides on the other side of the position where hydrolysis occurs (Figure 1). The small size and high speed (k_{obs} = 1 min^{-1}) of I-R3 have stimulated several applications.[31−33] A possible role of similar deoxyribozymes in sequence-specific genomic instability has also been suggested.[30] It has been reported that 15 nucleotides of the 17-nt core were highly conserved among the selected population. However, mutational analysis of I-R3 reported by Gu et al. was limited to A7T mutation, which abolished the activity, and that the substitution of A15 to any of the three other nucleotides or its deletion, which preserved catalytic function.[30] Therefore, it is unclear which nucleotides that constitute the 17-nt core of I-R3 tolerate mutations and the quantitative impacts of mutations on the catalytic activity.

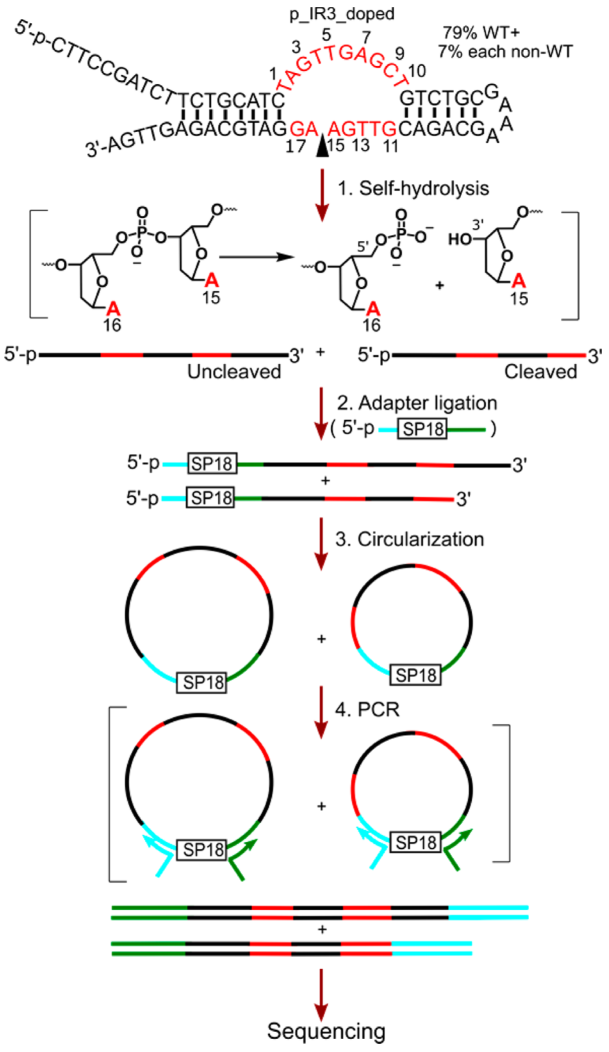

Figure 1. Sequence and structure of the deoxyribozyme I-R3 and outline of the library preparation process. The nucleotides that constitute the catalytic core are shown in red. The arrowhead indicates the cleavage site and "p" denotes 5′-phosphate group. Light blue and green lines indicate adapter sequences for deep sequencing. SP18 represents a hexa(ethylene glycol) spacer.

We adapted the comprehensive mutational analysis of ribozymes enabled by deep sequencing[28] to the self-hydrolyzing deoxyribozyme I-R3 to measure the activities of all possible single and double mutants of I-R3 at the core nucleotide positions 1 through 15 (Figure 1). As was the case with ribozymes, the key process is the construction of the sequencing library. A partially randomized deoxyribozyme library (p_IR3_doped, Table S1) was prepared in which the positions targeted for mutagenesis were synthesized by coupling 79% of the original (wild-type) base doped with 7% of each of the remaining three bases. As I-R3 is absolutely dependent on Zn^{2+} for its activity, premature cleavage and cleavage during library preparation were prevented by withholding Zn^{2+} or addition of excess EDTA. The resulting library was subjected to self-hydrolysis reaction in the reaction buffer (50 mM HEPES, pH 7.1, 2 mM $ZnCl_2$, 20 mM $MgCl_2$, 100 mM NaCl) at 37 °C for 1 h. Subsequently, an adapter oligonucleotide (p_adapter, Table S1) was ligated to the 5′ end of the reaction products (both cleaved and uncleaved) using T4 DNA ligase. The DNAs were then circularized by CircLigase and PCR amplified to yield the final library for deep sequencing (Figure 1). Deep sequencing requires attachment of fixed adapter sequences to both 5′ and 3′ ends of the DNA. Because the cleavage occurs on the 3′ side of the sequence that needs to be read, the adapter oligonucleotide (p_adapter) was ligated to the 5′ end, which is common to both cleaved and uncleaved DNAs, using T4 DNA ligase and a splint oligonucleotide. Because the 3′ ends of the DNAs are heterogeneous (due to cleavage and randomization), circularization was deemed to be more efficient[34] compared to nontemplated ligation of single-stranded DNAs.

Preservation of the relative yields of the cleaved and uncleaved DNA fragments directly affects the quality of the fraction cleaved (FC) values obtained by sequencing. Therefore, each step in the library construction was carefully monitored and optimized to minimize any bias introduced prior to sequencing. For example, we used a high-fidelity DNA polymerase and minimum number of thermal cycles (5 cycles) during PCR to minimize PCR biases. We also deliberately chose the 5′ end of the adapter (p_adapter, Table S1) to be guanine based on the substrate preference of CircLigase according to the manufacturer.

The raw reads from sequencing were filtered for quality using NGS QC Toolkit[35] and analyzed by custom Perl scripts. Each sequencing read identifies the mutant sequence of the original deoxyribozyme as well as its cleavage status. By counting the numbers of cleaved and uncleaved reads (N_{clv} and + N_{unclv}, respectively) for each mutant, fraction cleaved (FC) for each mutant can be calculated:

$$FC = N_{clv}/(N_{clv} + N_{unclv})$$

Where appropriate, FC was further normalized by that of the wild-type I-R3 (FC_{wt} = 0.82) and expressed as relative activity (RA). Deep sequencing yielded, on average, 24363 reads for each of the 45 single mutants and 2118 reads for each of the

DOI: 10.1021/acschembio.7b00621
ACS Chem. Biol. 2017, 12, 2940−2945

945 double mutants. Of the 12285 triple mutants, 7375 variants (60%) had at least 150 reads, which were sufficient for FC calculation (Table S2). I-R3 and 15 variants with varying FC values were chosen and individually assayed by conventional polyacrylamide gel electrophoresis (PAGE) to determine their activities (Table S3, Figure S1). FC values measured by the two methods showed an excellent linear correlation (Figure S1), validating the reliability of the sequencing based deoxyribozyme assay. The slope of 0.92 correlating the FC values by the two methods may be attributed to a minor bias introduced during the sequencing library preparation.

RA values of the 45 single and 945 double mutants are summarized in Figure 2, and the complete numerical data of these and 7375 (out of 12285 possible) triple mutants for which at least 150 reads were obtained are provided in Supplementary Data set.

A closer inspection of the RA values of the 45 single mutants (Figure 2A) reveals new observations regarding the sequence requirements of I-R3. As reported by Gu et al.,[30] A7T abolished catalytic activity, and all A15 substitutions were tolerated. Our results further revealed that G3, T5, G6, A7, G8, G11, T12, and G14 are critical for catalysis, with any substitution at these positions resulting in loss of activity. On the other hand, T4, C9, T10, T13, and A15 tolerate mutations. Although T1G retains activity, T1A results in a significant decrease in activity (RA = 0.25) and T1C is completely inactive, possibly due to base pairing with G17. A2G mutation is tolerated but not A2C or A2T. Although our library did not include mutants at A16 and G17, single mutants at these positions were examined by PAGE for completeness (Figure S2). Interestingly, all A16 mutants were active to some extent, while G17 mutants were all inactive.

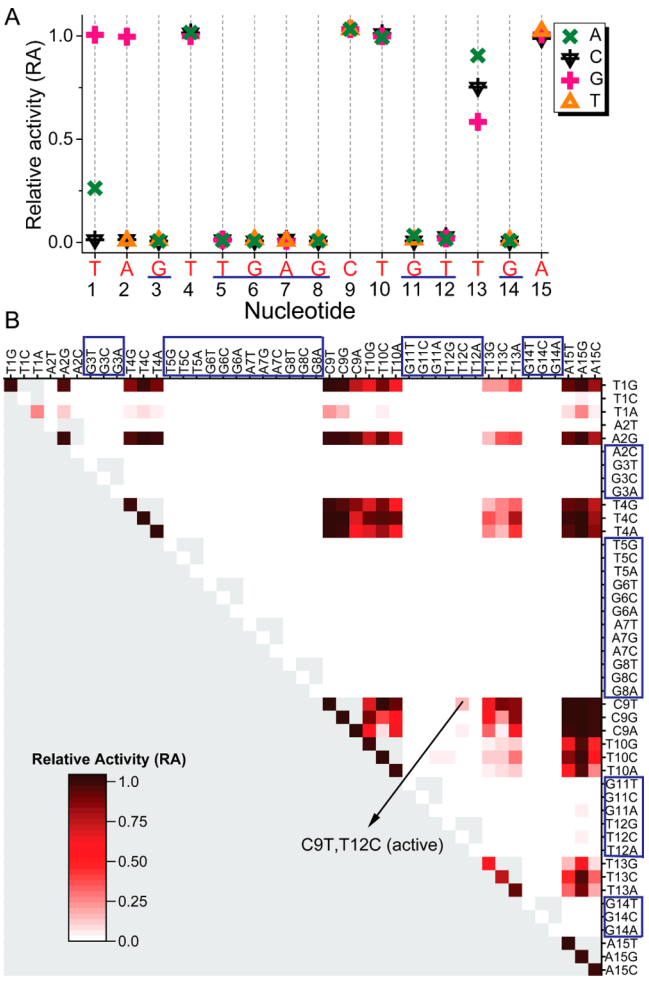

Figure 2. Relative activities (RAs) of single and double mutants of I-R3. (A) RA of 45 single mutants. The underlined nucleotides do not tolerate any mutations. (B) Two-dimensional RA matrix of all single and double mutants. Boxed nucleotides indicate mutations that inactive deoxyribozyme as single mutants. Single mutants appear on the diagonal side. The full RA matrix with numerical RA data is provided in Supplementary Data set.

Analysis of double mutants sometimes reveals covariable base pairs that are critical for structure and function. For example, if two single mutants result in loss of function but the combined double mutant restores function, it implies that those two bases may engage in functionally critical interactions. Our analysis of all 945 double mutants revealed no such potential interactions (Figure 2B). All double mutants that include a mutation that by itself inactivates the deoxyribozyme are inactive, except for T12C. Although T12C is inactive, the second mutation C9T partially restores activity (RA = 0.17, Figure 2B). Similarly, RA values of 7375 triple mutants with at least 150 reads confirmed that existence of one or more crippling mutations render the DNA catalytically inactive with the exception of few C9T/T12C mutants (Supplementary Data set).

The comprehensive mutational landscape of I-R3 based on our doped library implies a sharp fitness peak surrounding the wild-type (Figure S3). Our results indicate that the frequency of active mutants drops rapidly as more mutations accumulate. While 40% of single mutants retain RA > 0.2, 11.3% of all double mutants and 1.1% of triple mutants analyzed stay above the threshold (Table S4). The catalytically critical nucleotides are clearly identified, and any multiple base mutants that include one or more of the untolerated substitutions (Figure 2A) are likely to be inactive or marginally active. Therefore, we decided to explore higher-order mutants with combinations of tolerated single base substitutions according to Figure 2A. A new library p_IR3_revised (Figure 3A) was synthesized with the wild-type base, and where applicable, tolerated base substitutions with RA > 0.5 at each position. Seven nucleotides were varied with a total combination of 4096 sequences including the wild-type I-R3. Moreover, FC and RA values obtained from a reaction after a fixed time point are only semiquantitative. In particular, these values cannot differentiate reactions that are significantly faster than the sampling time scale. To gain a more quantitative understanding of the mutational landscape, the reaction of the new library was sampled at multiple time points so that a complete kinetic profile for each mutant could be acquired and be used to calculate observed rate constants (k_{obs}). Deep sequencing has been used to measure the binding kinetics of peptide ligands and a protein,[36] but no direct kinetic measurement of nucleic acid enzymes has been reported.

The library was analyzed similarly as described above with the exception of sampling the reaction at 1, 3, 8, 15, 30, 60, and 120 min. Samples from each time point were processed separately with unique barcodes but were combined prior to deep sequencing analysis. The kinetic data obtained by deep sequencing yielded sufficient read counts at each data point (Table S5 and Supplementary Data set). Additionally, reaction profiles of 11 deoxyribozymes were obtained by PAGE for comparison (Figure S4). Again, FC values calculated from the deep sequencing and PAGE assays showed an excellent

DOI: 10.1021/acschembio.7b00621
ACS Chem. Biol. 2017, 12, 2940−2945

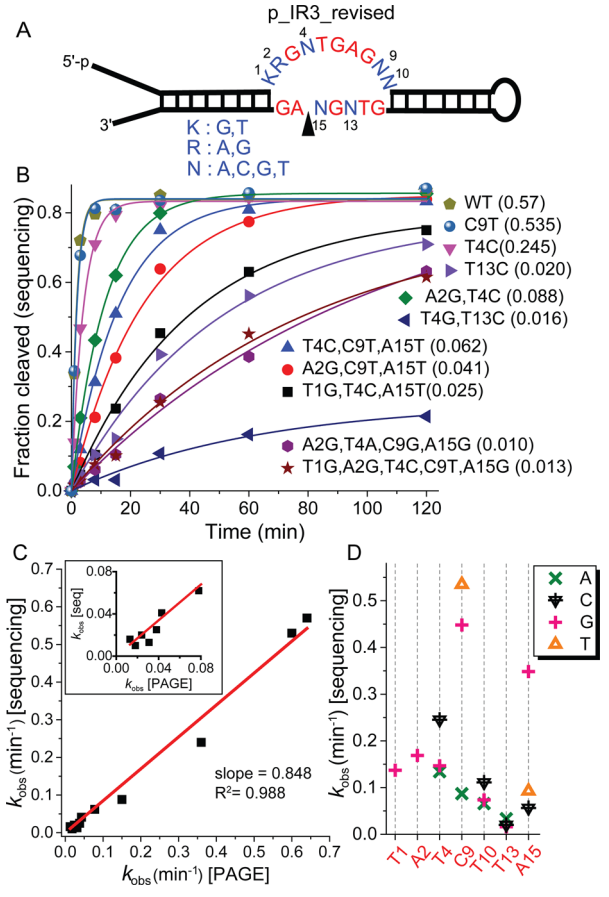

Figure 3. Kinetic analysis of I-R3 variants. (A) Targeted library of 4096 deoxyribozyme variants based on the tolerated substitutions in single mutant analysis. (B) Kinetic profiles of I-R3 and selected variants from the sequencing data. Values in parentheses represent k_{obs} derived from curve fit. (C) Correlation of k_{obs} values measured by conventional PAGE and sequencing assays. (D) Measured k_{obs} of single mutants by sequencing.

correlation (Figure S5A). Similarly, FC values of the single and double mutants after 1 h reaction from this library were plotted against the corresponding FC values from the original doped library (Figure S5B). The strong agreement of the two data sets obtained from two different libraries indicates good reproducibility of the deep sequencing assay.

Of the 4096 deoxyribozyme variants, 533 showed FC ≥ 0.20 after 2 h (Table S6) for which k_{obs} were calculated by fitting the reaction time course to the first-order kinetics (Figure 3B, Figure S6, and Supplementary Data set). The k_{obs} values calculated from the sequencing data agree well with those of 11 deoxyribozymes obtained by PAGE (Figure 3C and Table S7). For example, the k_{obs} of the wild-type based on the sequencing data is 0.57 min^{-1}, which is in close agreement with the PAGE based assay (0.64 min^{-1}) as well as that of the unimolecular I-R3 reported by Gu et al. (0.5 min^{-1}).[30] A closer look at the 17 single mutants revealed that while most variants showed RA ≈ 1.0 except for the three mutants at T13 (RA > 0.5) (Figure 2A), their k_{obs} values are significantly lower than the wild-type (Figure 3D). Notable exceptions include C9T (0.53 min^{-1}) and C9G (0.45 min^{-1}) whose k_{obs} values are comparable to that of the wild-type. Additionally, we found a large number of active higher-order mutants with as many as five mutations (quintuple mutants) with k_{obs} ranging from 0.015 to 0.002 min^{-1}, which are approximately 38- to 285-fold lower than k_{obs} of the wild-type (Figure S6). However, with no active mutants harboring more than five mutations identified, it is likely that we have analyzed most, if not all, functional I-R3 mutants in the vicinity of the wild-type sequence space. Based on the activity threshold of the mutants we analyzed (FC ≥ 0.20 after 2 h), we should have detected all variants with k_{obs} > ~0.002 min^{-1}.

Our findings are consistent with the view that I-R3 and its related functional mutants represent an isolated and narrow peak in the deoxyribozyme sequence space (Figure S3). An intriguing possibility suggested by Gu et al. of the small and active DNA self-hydrolysis motif represented by I-R3 is that there may be similar natural motifs in the genomes of organisms that may be subject to genomic instability.[30] They identified and tested several natural motifs in vitro and confirmed their activity. Although the biological relevance of I-R3 related motifs remains inconclusive, comprehensive and quantitative sequence requirements of deoxyribozymes that our method affords should help identify potentially catalytic DNA motifs in natural genomes.

Availability of k_{obs} for a large set of mutants provides new opportunities to understand the mutational effects of the deoxyribozyme at a more quantitative level. Here, we consider the k_{obs} of a double mutant (k_{ij}) and those of the respective single mutants (k_i and k_j). If the two mutations are independent, that is, if each mutation affects the activation energy (E_a) of the reaction in an additive manner, the Arrhenius equation predicts that

$$k_{ij\_rel} = k_{i\_rel} \cdot k_{j\_rel}$$

where k_{i_rel} signifies relative k_{obs} normalized by k_{obs} of the wild-type (Supporting Information, methods). Inequality of k_{ij_rel} and $k_{i\_rel} \cdot k_{j\_rel}$ implies either positive or negative epistasis, or coupling of the two mutations. For example, $k_{ij\_rel} > k_{i\_rel} \cdot k_{j\_rel}$ shows antagonistic epistasis in which the double mutant is more active than if the two single mutations were to affect the activity (E_a) in an additive manner. We plotted k_{ij_rel} vs $k_{i\_rel} \cdot k_{j\_rel}$ of all 105 double mutants for which measurable k_{obs} were obtained (Figure 4A). The plots indicate that most of the double mutations appear to show weak or no epistasis, but it also highlights exceptions that would have been difficult to detect without such analysis. We identified only 9 mutants whose k_{ij_rel} and $k_{i\_rel} \cdot k_{j\_rel}$ differ by 3-fold or more (Figure 4). The relative magnitude of epistasis of each mutant can be more quantitatively represented as follows (eq 12 in Methods):

$$\Delta\Delta E_{ij} = (\Delta E_i + \Delta E_j) - \Delta E_{ij}$$

where ΔE_i, ΔE_j, and ΔE_{ij} are the increases in the activation energy relative to the wild-type. These values can be calculated from the relative rate constant k_{i_rel}, etc.:

$$\Delta E_i = -RT \ln k_{i\_rel}$$

Distribution of $\Delta\Delta E_{ij}$ values of the 105 double mutants (Figure 4B,C) again shows that majority of the mutations show weak or no epistasis. Few notable exceptions include T13C, A15C showing the highest $\Delta\Delta E_{ij}$ and C9G, T10C with strong synergistic epistasis (negative $\Delta\Delta E_{ij}$) (Figure 4C). Although based on single time-point assays, our recent mutational study of a natural twister ribozyme indicated a number of epistatic interactions consistent with the crystal structure as well as mutational robustness.[28] However, the size of the naturally evolved ribozyme is significantly larger. The compactness of the

DOI: 10.1021/acschembio.7b00621
ACS Chem. Biol. 2017, 12, 2940−2945

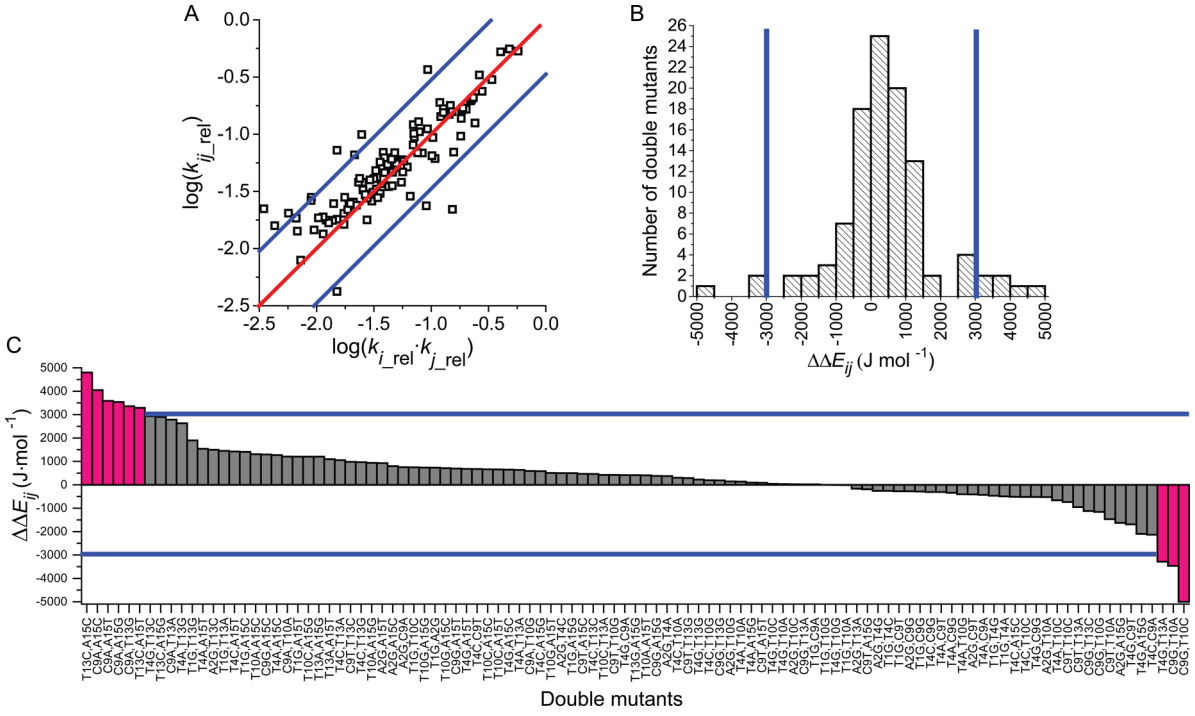

Figure 4. Epistatic analysis of 105 double mutants (*ij*). The data points and bar graphs shown within blue lines are in within 3-fold noise range. (A) Correlation between the relative rate constants of double mutants (k_{ij_rel}) and the product of their respective single mutants (k_{i_rel}·k_{j_rel}) in log scale. The red line is $y = x$ which corresponds to no epistasis ($\Delta\Delta E_{ij} = 0$, $k_{ij\_rel} = k_{i\_rel}$·k_{j_rel}). The blue lines indicate $y = 3x$ and $y = x/3$, between which k_{ij_rel} and k_{i_rel}·k_{j_rel} are within 3-fold range. (B) Distribution of $\Delta\Delta E_{ij}$ values of the double mutants. (C) Calculated $\Delta\Delta E_{ij}$ values of 105 double mutants with measurable rate constants.

catalytic core of I-R3 may have resulted in a more restrictive sequence requirement and fewer epistatic interactions.

As demonstrated in this work, we used deep sequencing to obtain a quantitative overview of the sequence−function relationship of a deoxyribozyme that would not have been possible using conventional assays. With appropriate modifications of the sequencing library preparation procedure, large scale deoxyribozyme assay by deep sequencing should serve as a powerful methodology to deepen our understanding of various deoxyribozymes as well as to engineer them for practical applications.

■ ASSOCIATED CONTENT

Supporting Information

The Supporting Information is available free of charge on the ACS Publications website at DOI: 10.1021/acschembio.7b00621.

List of DNA oligonucleotides used for library preparation, experimental methods, summary of deep sequencing statistics, cleavage activities of selected mutants, validation of sequencing results by PAGE experiments, activities of mutants at positions 16 and 17, distribution of mutant activities, kinetic plots, and k_{obs} of selected variants (from PAGE and sequencing) (PDF)

Data set containing N_{clv}, N_{unclv}, FC, and RA values of I-R3 mutants, RA matrix shown in Figure 2B with RA values, and the activity data for the kinetic analysis (XLSX)

■ AUTHOR INFORMATION

Corresponding Author

*E-mail: yohei.yokobayashi@oist.jp.

ORCID

V. Dhamodharan: 0000-0002-5249-8096

Shungo Kobori: 0000-0003-4995-5847

Yohei Yokobayashi: 0000-0002-2417-1934

Notes

The authors declare no competing financial interest.

■ ACKNOWLEDGMENTS

The authors thank H. Goto and OIST DNA Sequencing Section for sequencing support. This work was supported by Okinawa Institute of Science and Technology Graduate University.

■ REFERENCES

(1) Silverman, S. K. (2016) Catalytic DNA: Scope, Applications, and Biochemistry of Deoxyribozymes. *Trends Biochem. Sci. 41*, 595−609.

(2) Hollenstein, M. (2015) DNA Catalysis: The Chemical Repertoire of DNAzymes. *Molecules 20*, 20777−20804.

(3) Chandra, M., Sachdeva, A., and Silverman, S. K. (2009) DNA-catalyzed sequence-specific hydrolysis of DNA. *Nat. Chem. Biol. 5*, 718−720.

(4) Breaker, R. R., and Joyce, G. F. (1994) A DNA enzyme that cleaves RNA. *Chem. Biol. 1*, 223−229.

(5) Brandsen, B. M., Hesser, A. R., Castner, M. A., Chandra, M., and Silverman, S. K. (2013) DNA-Catalyzed Hydrolysis of Esters and Aromatic Amides. *J. Am. Chem. Soc. 135*, 16014−16017.

(6) Chandra, M., and Silverman, S. K. (2008) DNA and RNA can be equally efficient catalysts for carbon−carbon bond formation. *J. Am. Chem. Soc. 130*, 2936−2937.

(7) Silverman, S. K. (2008) Catalytic DNA (deoxyribozymes) for synthetic applications-current abilities and future prospects. *Chem. Commun.*, 3467−3485.

DOI: 10.1021/acschembio.7b00621
ACS Chem. Biol. 2017, 12, 2940−2945

(8) Höbartner, C., and Pradeepkumar, P. I. (2012) DNA Catalysts for Synthetic Applications in Biomolecular Chemistry, *New Strategies in Chemical Synthesis and Catalysis*, pp 129−155, Wiley-VCH.
(9) Torabi, S.-F., Wu, P., McGhee, C. E., Chen, L., Hwang, K., Zheng, N., Cheng, J., and Lu, Y. (2015) In vitro selection of a sodium-specific DNAzyme and its application in intracellular sensing. *Proc. Natl. Acad. Sci. U. S. A. 112*, 5903−5908.
(10) Ponce-Salvatierra, A., Wawrzyniak-Turek, K., Steuerwald, U., Höbartner, C., and Pena, V. (2016) Crystal structure of a DNA catalyst. *Nature 529*, 231−234.
(11) Zaborowska, Z., Fürste, J. P., Erdmann, V. A., and Kurreck, J. (2002) Sequence Requirements in the Catalytic Core of the "10−23" DNA Enzyme. *J. Biol. Chem. 277*, 40617−40622.
(12) Peracchi, A., Bonaccio, M., and Clerici, M. (2005) A Mutational Analysis of the 8−17 Deoxyribozyme Core. *J. Mol. Biol. 352*, 783−794.
(13) Zaborowska, Z., Schubert, S., Kurreck, J., and Erdmann, V. A. (2005) Deletion analysis in the catalytic region of the 10−23 DNA enzyme. *FEBS Lett. 579*, 554−558.
(14) Schlosser, K., Gu, J., Sule, L., and Li, Y. (2008) Sequence-function relationships provide new insight into the cleavage site selectivity of the 8−17 RNA-cleaving deoxyribozyme. *Nucleic Acids Res. 36*, 1472−1481.
(15) Wang, B., Cao, L., Chiuman, W., Li, Y., and Xi, Z. (2010) Probing the Function of Nucleotides in the Catalytic Cores of the 8−17 and 10−23 DNAzymes by Abasic Nucleotide and C3 Spacer Substitutions. *Biochemistry 49*, 7553−7562.
(16) Wachowius, F., Javadi-Zarnaghi, F., and Höbartner, C. (2010) Combinatorial mutation interference analysis reveals functional nucleotides required for DNA catalysis. *Angew. Chem., Int. Ed. 49*, 8504−8508.
(17) Wachowius, F., and Höbartner, C. (2011) Probing essential nucleobase functional groups in aptamers and deoxyribozymes by nucleotide analogue interference mapping of DNA. *J. Am. Chem. Soc. 133*, 14888−14891.
(18) Samanta, B., and Höbartner, C. (2013) Combinatorial Nucleoside-Deletion-Scanning Mutagenesis of Functional DNA. *Angew. Chem., Int. Ed. 52*, 2995−2999.
(19) Javadi-Zarnaghi, F., and Höbartner, C. (2016) Functional Hallmarks of a Catalytic DNA that Makes Lariat RNA. *Chem. - Eur. J. 22*, 3720−3728.
(20) Curtis, E. A., and Bartel, D. P. (2013) Synthetic shuffling and in vitro selection reveal the rugged adaptive fitness landscape of a kinase ribozyme. *RNA 19*, 1116−1128.
(21) Hayden, E. J., and Wagner, A. (2012) Environmental change exposes beneficial epistatic interactions in a catalytic RNA. *Proc. R. Soc. London, Ser. B 279*, 3418−3425.
(22) Pitt, J. N., and Ferré-D'Amaré, A. R. (2010) Rapid Construction of Empirical RNA Fitness Landscapes. *Science 330*, 376−379.
(23) Ameta, S., Winz, M.-L., Previti, C., and Jäschke, A. (2014) Next-generation sequencing reveals how RNA catalysts evolve from random space. *Nucleic Acids Res. 42*, 1303−1310.
(24) Pressman, A., Moretti, J. E., Campbell, G. W., Müller, U. F., and Chen, I. A. (2017) Analysis of in vitro evolution reveals the underlying distribution of catalytic activity among random sequences. *Nucleic Acids Res. 45*, 8167−8179.
(25) Jiménez, J. I., Xulvi-Brunet, R., Campbell, G. W., Turk-MacLeod, R., and Chen, I. A. (2013) Comprehensive experimental fitness landscape and evolutionary network for small RNA. *Proc. Natl. Acad. Sci. U. S. A. 110*, 14984−14989.
(26) Niland, C. N., Zhao, J., Lin, H.-C., Anderson, D. R., Jankowsky, E., and Harris, M. E. (2016) Determination of the Specificity Landscape for Ribonuclease P Processing of Precursor tRNA 5′ Leader Sequences. *ACS Chem. Biol. 11*, 2285−2292.
(27) Kobori, S., Nomura, Y., Miu, A., and Yokobayashi, Y. (2015) High-throughput assay and engineering of self-cleaving ribozymes by sequencing. *Nucleic Acids Res. 43*, e85.
(28) Kobori, S., and Yokobayashi, Y. (2016) High-Throughput Mutational Analysis of a Twister Ribozyme. *Angew. Chem., Int. Ed. 55*, 10354−10357.
(29) Kobori, S., Takahashi, K., and Yokobayashi, Y. (2017) Deep Sequencing Analysis of Aptazyme Variants Based on a Pistol Ribozyme. *ACS Synth. Biol. 6*, 1283−1288.
(30) Gu, H., Furukawa, K., Weinberg, Z., Berenson, D. F., and Breaker, R. R. (2013) Small, highly active DNAs that hydrolyze DNA. *J. Am. Chem. Soc. 135*, 9121−9129.
(31) Gu, H., and Breaker, R. R. (2013) Production of single-stranded DNAs by self-cleavage of rolling-circle amplification products. *BioTechniques 54*, 337−343.
(32) Furukawa, K., and Minakawa, N. (2014) Allosteric control of a DNA-hydrolyzing deoxyribozyme with short oligonucleotides and its application in DNA logic gates. *Org. Biomol. Chem. 12*, 3344−3348.
(33) Endo, M., Takeuchi, Y., Suzuki, Y., Emura, T., Hidaka, K., Wang, F., Willner, I., and Sugiyama, H. (2015) Single-Molecule Visualization of the Activity of a Zn2+-Dependent DNAzyme. *Angew. Chem., Int. Ed. 54*, 10550−10554.
(34) Heyer, E. E., Ozadam, H., Ricci, E. P., Cenik, C., and Moore, M. J. (2015) An optimized kit-free method for making strand-specific deep sequencing libraries from RNA fragments. *Nucleic Acids Res. 43*, e2.
(35) Patel, R. K., and Jain, M. (2012) NGS QC Toolkit: A Toolkit for Quality Control of Next Generation Sequencing Data. *PLoS One 7*, e30619.
(36) Jalali-Yazdi, F., Huong Lai, L., Takahashi, T. T., and Roberts, R. W. (2016) High-Throughput Measurement of Binding Kinetics by mRNA Display and Next-Generation Sequencing. *Angew. Chem., Int. Ed. 55*, 4007−4010.

DOI: 10.1021/acschembio.7b00621
ACS Chem. Biol. 2017, 12, 2940−2945